Journal of Coastal and Marine Engineering
Volume 1 • Number 1 • June 2018

Numerical Analysis of Upheaval Buckling of Pipeline on Uneven Seabed Using Finite Element Method

Ali Soukhak Lari[1*], Ahmad Rahbar Ranji[2], Mostafa Bahmani Shoorijeh[3] and Mehdi Soukhak Lari[4]

1) Maritime Engineering Department, Amirkabir University of Technology, Tehran, Iran, asl61@aut.ac.ir
2) Maritime Engineering Department, Amirkabir University of Technology, Tehran, Iran, rahbar@aut.ac.ir
3) Zachry Department of Civil Engineering, Texas A&M University, Texas, USA, bahm64@tamu.edu
4) Maritime Engineering Department, Amirkabir University of Technology, Tehran, Iran, mehdi.soukhak@aut.ac.ir

Abstract: c

Keywords: Numerical analysis, Subsea Pipeline, Initial Imperfection, Upheaval Buckling, FEM.

1. Introduction

In recent years, application of offshore pipelines has increased due to increase in energy demand in industries as well as the need to explore new oil and gas fields. This energy demand has made explorations for new hydrocarbon sources to be concentrated in the deep waters. Production and discovery of oil and gas in the deep waters requires long pipelines. More importantly, the design of these pipelines has generated many challenges for big corporations and engineers.

Pipelines play significant role in offshore transportation system. Presently, it is the cheapest and the best way of transporting hydrocarbons from deep waters to the shore and refineries without contamination by the sea environment.

In accordance with DNV-RP-F110 [1], in deep water and on the uneven seabed, there are two types of buckling possibility; lateral buckling and upheaval buckling. These two types of buckling have been identified as types of global buckling. Upheaval buckling can also occur in buried situation or in the trench.

In deep water, by imposing the initial imperfection and increasing the temperature and internal pressure, axial compressive stress develops on the pipeline wall thickness and the shape of the pipeline is changed when the compression load is more than the soil resistance. Subsequently, this compression axial stress will induce the release of an internal accumulated stress that is caused by interaction between the pipeline and seabed.

Many researchers have investigated this topic and obtained good results, but all of them have neglected one or some parameters for simulation and analysis due to easier methods of analysis. Hobbs [2] suggested some lateral buckling modes and derived analytical solution for both upheaval and lateral buckling of pipelines in relation to critical axial force, buckling amplitude and length. Taylor and Gan [3] derived analytical solution of first and second order on the basis of an initial imperfection in the pipelines. Wang et al. [4, 5] studied upheaval buckling of pipelines with soft seabed. They considered the effects of initial imperfection and soil friction coefficient on the pipeline. Liu et al. [6, 7] investigated the effects of thermal stress and temperature differences on lateral and upheaval modes employing analytical and numerical techniques such as finite element models. Zeng et al. [8] proposed three different formulae for simulating initial imperfection in upheaval buckling based on a finite element method on the rigid seabed. Zhang et al. [9] worked on critical axial force of upheaval buckling under different shape of out-of-straightness and initial imperfections on the basis of finite element models.

All of the above studies considered the analysis of a rigid seabed, but an actual seabed is deformable. In this research, an attempt was made to verify the upheaval buckling of pipelines on the uneven and deformable seabed under various soil friction coefficients employing ABAQUS software. Several parameters including pipeline length, pipeline weight, external and internal pressure, initial imperfection and operating temperature were considered.

2. Global Buckling

The exposed pipelines on the uneven seabed have potential of undergoing global buckling under high axial compressive forces or low buckling bearing capacity. The impacts of temperature and pressure generate the efficacious expansion forces that create global buckling in the pipeline. When the buckling occurs in the pipeline, a part of restricted thermal expansion is released and consequently, the compressive force at the buckled section of the pipeline is diminished. The effective axial force is the triggering force for initiation of the global buckling. As a matter of fact, this force is derived from the combination activity of the wall thickness force and the internal and external pressure.

2.1. Verification of the Probabilities of Occurrence of the Global Buckling

*Corresponding author.

On the basis of DNV-RP-F110 [1], the objective of this section is to evaluate the probabilities of global buckling. The axial load global resistance or capacity depends on the lateral load e.g. trawl impact, lateral resistance and geometrical imperfection of the global configuration as shown in Figure 1. Depending on the susceptibility, different criteria are "No Buckling, Maybe Buckling and Buckling".

When the axial force induced by high temperature and pressure in the pipeline rises to the ultimate axial force, the pipeline is buckled. In this situation, the axial force attains its maximum value. If the axial force in the pipeline is less than the ultimate value, the buckling will not occur in the pipeline. Between these two aforementioned cases, in the event that the pipeline is under accidental loads such as trawling load induced by the ship's anchor, the buckling will occur.

To determine the effective axial force for upheaval buckling mode in the pipeline, DNV-RP-F110 [1] has proposed following linear equation based on a prop shape model:

$$S_{eff} = (R_{\max} + W_p + k_2.W_o)\sqrt{\frac{EI}{k_1^2.\delta.W_o}} \quad (1)$$

where S_{eff} is the effective axial force, $R_{\max}$ is the total soil resistance (or the friction force per unit length of pipe), W_o is the submerged weight of the pipe during installation, W_p is the submerged weight of pipe during operation, δ is the (prop) imperfection, EI is the bending stiffness, $k_1 = 2$ and $k_2 = 11$ are constant determined from FE results for prop shape scenarios.

Since actual distribution of normal force is hard to determine, for the purpose of friction force calculation, a simplified model can be employed to determine $R_{\max}$. For an unburied pipeline, the soil force or soil resistance is given by [10]:

$$R_{\max} = \mu(W_d - F_b) \quad (2)$$

where μ is coefficient of friction for soil, W_d is dry weight of the pipe and contents (or weight per unit length of pipe), F_b is buoyant force in per unit length of pipe.

Eq. (1) has its limitation and should preferably be used only at the conceptual design phase. Typical limitations include:

- permits only linear elastic material behavior
- difficult to describe an arbitrary imperfection shape
- soil upheaval resistance is assumed along the entire imperfection wavelength. This is not the case in sag band regions, where the pipeline will have a propensity to move downwards, resulting in no soil contribution to uplift resistance.
- does not take the vertical soil resistance force-displacement curve into account
- cannot account for cyclic loading and possible creep.

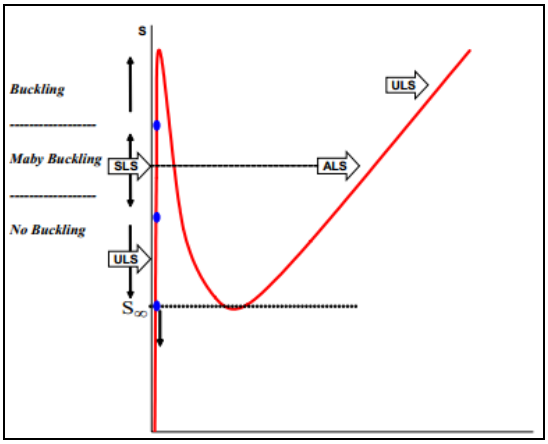

Figure 1. The different situations of buckling probabilities

3. Finite Element Model

All of the elements in this research are simulated using 3D framework (Figure 2). All properties are also selected based on Persian Gulf situations. The analyses in this paper are fulfilled based on CEL/ Dynamic Implicit technique employing ABAQUS software, version 6.13 for analysis of pipeline buckling. Moreover, the analysis procedure is determined in five major steps; the gravity force, initial imperfection, external and internal pressure, and finally operational temperature are exerted on the model, respectively.

Soil type of seabed is "Silty Clays", and the Mohr Coulomb criterion is considered to similar the soil behavior. The C3D8R element is used for meshing the soil with 1 m dimensions in X and Y directions, and 0.5 m dimension in Z direction. The dimensions of soil model are as follow: 6 m in X direction, 1000 m in Y direction and 3 m in Z direction. For the boundary conditions, it is tried to constraint all directions at the bottom of The FEA model, while for the lateral sides; only X and Y directions are restricted. Other parameters are tabulated in Table 1.

The PIPE31 element is considered to have a mesh with 1 m long. An elastic behavior model for simulation of the pipe behavior is also applied. The properties of the pipeline include length of 1000 m, diameter of 323.9 mm, wall thickness of 12.7 mm from API 5L X65 grade. Other details are presented in Table 2.

The "contact properties" between pipeline and seabed are considered as "Tangential and Normal Behavior". In tangential behavior, the friction behavior is "Penalty" type and the friction coefficient is set at 0.1 to 0.4 for each analysis, respectively, and normal behavior is defined by "Hard" contact.

Operational characteristics include water depth of 70 m, operating temperature of 120 ℃ and internal pressure of 10 MPa. In addition, in order to carry out the analysis, other variable parameters are applied as follow:

- Soil friction coefficient (μ): 0.1, 0.2, 0.3, 0.4
- Initial imperfection amplitude (V_o): 100 cm
- Imperfection length (L_o): 100 m

The initial imperfection can be created as shown in Figure 3 employing the equation below (Zeng and et al. [8]):

$$f(x)=\frac{V_o}{2}\left(1+\cos\left(\frac{2\pi x}{L_o}\right)\right),\quad \frac{-L_o}{2}\le x\le\frac{L_o}{2} \tag{3}$$

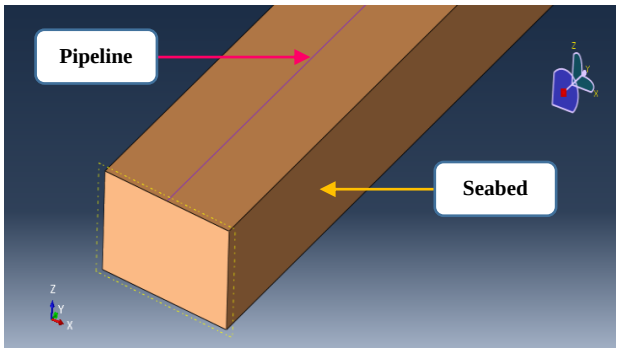

Figure 2. Numerical modeling of pipeline and seabed.

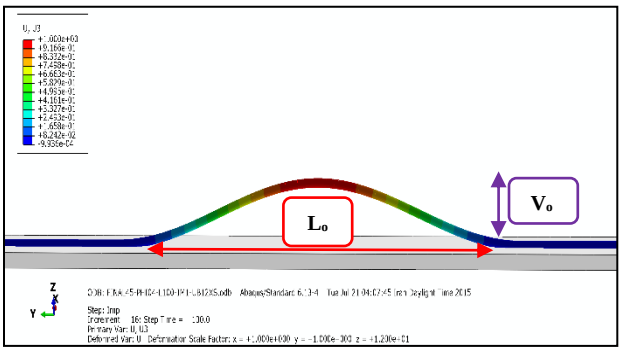

Figure 3. Creation of initial imperfection in the pipeline.

Table 1. Seabed properties.

Elasticity Modulus E_{Soil} (N/m^2)	Mass Density ρ (Kg/m^3)	Poisson's Ratio ν	Internal Friction Angle $\varphi(°)$	Cohesion C (N/m^2)
5.5×10^6	1960	0.3	25	20000

Table 2. Pipeline properties.

Elasticity Modulus E_{Steel} (N/m^2)	Mass Density $\rho(Kg/m^3)$	Poisson's Ratio ν	Thermal Expansion Coefficient $\alpha(℃^{-1})$	Minimum Yield Stress σ_y (N/m^2)
2.06×10^{11}	7850	0.3	1.16×10^{-5}	450×10^6

4. Analysis of the Results

The sensitivity of upheaval buckling with respect to changing of the operating temperature and the friction coefficient between soil and pipeline was investigated by considering four different magnitude of μ. As previously mentioned, the initial imperfection in the middle of the pipeline and the imperfection length was considered to be 100 cm and 100 m, respectively.

The variations in displacement induced by increase in the friction coefficient are shown in Figure 4. As μ increases from 0.1 to 0.4, the displacement at the end of the curves decreases, although the difference between the curves is very low. This indicates that an easier displacement would occur in the middle of the pipeline with a smaller soil friction coefficient. The oscillations and their frequencies are also similar in the curves. Consequently, because of the friction between seabed and the pipeline, these fluctuations are damped, and they are made to converge on the straight lines. Table 3 shows all details about the end of displacement in all diagrams.

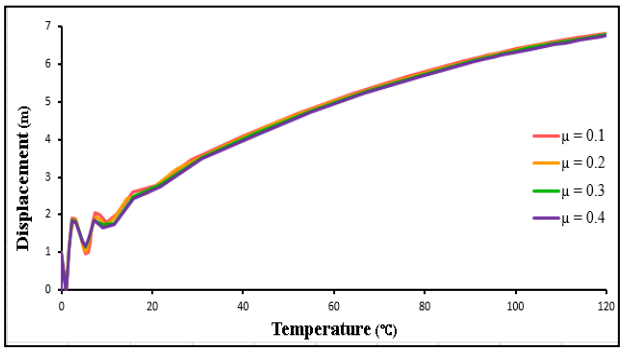

Figure 4. Displacements in the middle of pipeline

Table 3. The values of maximum displacement.

Soil friction coefficient (μ)	Maximum Displacement (m)
0.1	6.83
0.2	6.81
0.3	6.78
0.4	6.75

It can be seen in Figure 5 that the increase in μ from 0.1 to 0.4 have a great influence on the effective axial force, and this force is augmented in the supports and the middle of pipeline. As a matter of fact, this shows that whenever μ is on the verge of increase, deformation of the middle point due to increase in friction between the soil and the pipeline would be more difficult. Consequently, the level of the stored potential energy is increased. For more clarification, when μ is 0.1, the effective axial force in the middle and the supports are -222539 N and -270158 N, respectively. When μ attains to 0.4, the effective axial force in the middle and the supports increase to -224648 N and -414845 N, respectively, which shows 0.95% and 53.6% expansion. Furthermore, the pipeline will be unstable when the effective axial force rises. These values are obtained easily, as illustrated in Table 4.

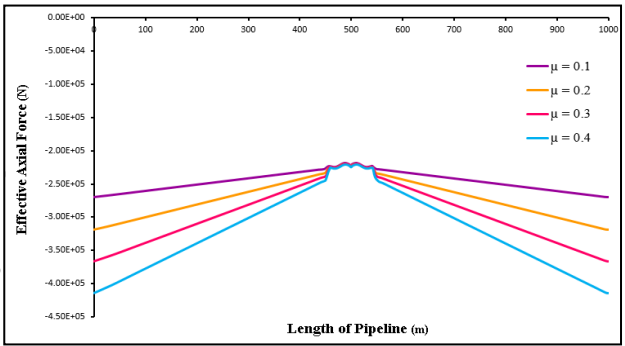

Figure 5. Effective axial force in the pipeline

Table 4. The values of effective axial force.

Soil friction coefficient (μ)	Supports of the pipeline (N)	Middle of the pipeline (N)
0.1	-270158	-222539
0.2	-318378	-223216
0.3	-366377	-223715
0.4	-414845	-224648

Table 5. The values of R_{max} and S_{eff}.

Soil friction coefficient (μ)	Total soil resistance (R_{max}) (N)	Effective axial force (S_{eff}) (N)
0.1	-14.80	-1097703
0.2	-29.60	-1099117
0.3	-44.40	-1100530
0.4	-59.20	-1101944

As for Eq. (1) and Eq. (2), the values of R_{max} and S_{eff} for the four soil friction coefficient in the pipeline are shown in Table 5. According to Table 4 and 5, it is clearly evident that the limit of stability of the pipeline depends on the final limit of the effective axial force or S_{eff}. Actually, by gradually increasing the operating temperature and the soil friction coefficient, the effective axial force is increased in the pipeline. Whenever this augmentation would be greater, the value of the effective axial force would increase. This augmentation can also be continued until S_{eff} is attained, then the pipeline would experience a failure in that segment. In all states of the analysis, S_{eff} are greater than the values in Table 4. Thus in this research, the pipeline remains at an allowable range without fracture.

Figure 6 shows the effective axial force in the middle of the pipeline. Based on this Figure, when the temperature rises from 0 to 120℃, some oscillations are generated at the beginning of the process. These oscillations exist until attainment of 20℃. However, after 20℃, the fluctuations disappear by gradually damping the effects of the soil. Eventually, these diagrams are converged on the partly straight directions. According to Table 4, it is obvious that by increasing the soil friction coefficient, the values of the effective axial force in the middle of pipeline increase.

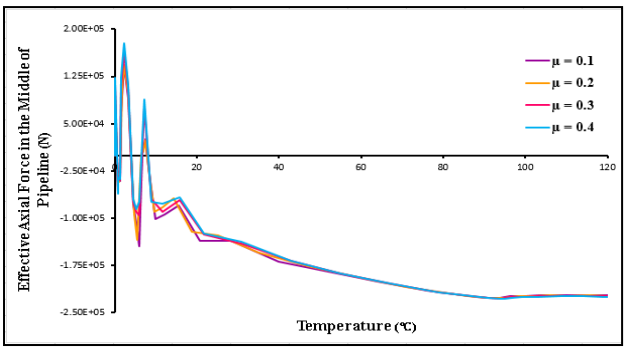

Figure 6. Effective axial force in the middle of pipeline

In accordance with Table 6, the values show changes in bending moment in the pipeline. By increasing of the soil friction coefficient, the maximum positive and maximum negative values of bending moment diminish near the middle of pipeline. The maximum absolute moments are also in the positive parts of the values. Moreover, moments of the fix end (the bending moment in the supports) are not zero, and these values are almost similar.

Table 6. The values of bending moment.

Soil friction coefficient (μ)	Moment of the fix end (N m)	Maximum positive moment (N m)	Maximum negative moment (N m)
0.1	3143.62	537869	-395239
0.2	3144.37	537748	-394637
0.3	3145.12	537225	-393765
0.4	3145.75	537180	-393550

5. Conclusions

For the numerical solution, an attempt was made to investigate the upheaval buckling of pipeline. Consequently, an FEA model with initial imperfection and various soil friction coefficient on the deformable seabed was established for simulation of the upheaval buckling, and some results were derived as follow:

1- The results show that by increasing the soil friction coefficient, displacement and the bending moment are reduced and the effective axial force in the middle and whole pipeline increase in the pipeline. This is due to the increase in the resistant of the forces against the expansion of the pipeline displacement. Afterwards, the level of the energy is developed continuously. This indicates that the changes in soil friction has a significant impact on the upheaval buckling of the pipeline.

2- The stability of the pipeline is defined by S_{eff} with respect to the effective axial force generated in the pipeline. As the soil friction coefficient and operational temperature are changed, the effective axial force at the supports and the middle of pipeline become smaller than S_{eff}. Hence, the pipeline is kept in a safe range without any fracture.

6. References

[1] Veritas, D. N. "Global buckling of submarine pipelines–structural design due to high temperature/high pressure." *Prática Recomendada, DNV RP-F110*, 2007,

[2] Hobbs, R. E. "In-service buckling of heated pipelines." *Journal of Transportation Engineering*, 2, 1984, pp. 175-189.

[3] Taylor, N.andGan, A. B. "Submarine pipeline buckling—imperfection studies." *Thin-Walled Structures*, 4, 1986, pp. 295-323.

[4] Wang, L., Shi, R., Yuan, F., Guo, Z.andYu, L. "Global buckling of pipelines in the vertical plane with a soft seabed." *Applied Ocean Research*, 2, 2011, pp. 130-136.

[5] Shi, R., Wang, L., Guo, Z.andYuan, F. "Upheaval buckling of a pipeline with prop imperfection on a plastic soft seabed." *Thin-Walled Structures*, 2013, pp. 1-6.

[6] Guo, L.-p., Liu, R.andYan, S.-w. "Global buckling behavior of submarine unburied pipelines under thermal stress." *Journal of Central South University*, 7, 2013, pp. 2054-2065.

[7] Liu, R., Wang, W.-g.andYan, S.-w. "Finite element analysis on thermal upheaval buckling of submarine burial pipelines with initial imperfection." *Journal of Central South University*, 1, 2013, pp. 236-245.

[8] Zeng, X., Duan, M.andChe, X. "Critical upheaval buckling forces of imperfect pipelines." *Applied Ocean Research*, 2014, pp. 33-39.

[9] Zhang, X.andDuan, M. "Prediction of the upheaval buckling critical force for imperfect submarine pipelines." *Ocean Engineering*, 2015, pp. 330-343.

[10] Guo, B., Song, S., Ghalambor, A.andChacko, J. *Offshore pipelines*. Elsevier, 2005.